Anal. Bioanal. Electrochem., Vol. 9, No. 6, 2017, 741-761

Analytical & Bioanalytical Electrochemistry

2017 by CEE
www.abechem.com

Full Paper

A New Sensor Based on the Glassy Carbon Electrode Modified with Poly Aspartic Acid-Fe_3O_4 Nanoparticle/ Multi-Walled Carbon Nanotubes Composite for a Selective Simultaneous Determination of Piroxicam and Clopidogrel in the Presence of Uric Acid

Ali Babaei,[1,2,*] Mohammad Afrasiabi[1] and Hassan Moghanian[3]

[1]*Department of Chemistry, Faculty of Science, Arak University, Arak, I.R. Iran*
[2]*Institute of Nanosciences & Nanotechnology, Arak University, Arak, I.R. Iran*
[3]*Department of Chemistry, Dezful Branch, Islamic Azad University, Dezful, I.R. Iran*

*Corresponding Author, Tel.: +98 863 4173401; Fax: +98 863 4173406
E-Mail: ali-babaei@araku.ac.ir

Received: 2 December 2016 / Accepted with minor revision: 2 August 2017/ Published online: 30 September 2017

Abstract- A novel modified glassy carbon electrode based on poly aspartic acid-Fe_3O_4 nanoparticle / multi-walled carbon nanotubes composite (PAA-FeNPs-MWCNTs/GCE) was developed and used as an efficient sensor for simultaneous determination of piroxicam (PRX) and clopidogrel (CLO) in the presence of uric acid (UA). Response surface methodology (RSM) was utilized in optimization of the effects of various operating variables on the voltammetric response of PRX and CLO suggesting that the amount of PAA-FeNPs in the modifier matrix (% PAA-FeNPs), the solution pH and the accumulation time (t) were the three most important operating factors. The central composite design (CCD) as a response surface approach was applied for obtaining the optimum conditions as well as the maximum heights for oxidation peak currents of PRX and CLO. The differential pulse voltammetry (DPV) results showed that under the optimal experimental conditions the obtained anodic peak currents were linearly proportional to concentration in the range of 0.2-80 µM with a detection limit (S/N = 3.0) of 45 nM for PRX and in the range of 0.4-48 µM and with a detection limit of 76 nM for CLO. The applicability of the proposed method was successfully demonstrated for simultaneous determination of these compounds in human urine and blood serum samples.

Keywords- Piroxicam, Clopidogrel, Central composite design, Electrochemical sensors, Multi-walled carbon nanotubes, Poly aspartic acid-Fe_3O_4 nanoparticle

1. INTRODUCTION

As are allotropes of carbon with a cylindrical nanostructure, carbon nanotubes (CNTs) have been synthesized with length-to-diameter ratio which is significantly larger than any other material. Such an extraordinary structure gives them unique properties including high electrical conductivity, great chemical stability and extreme mechanical strength which make them potentially useful as a modifier in various sensors [1-6].

The extraordinary chemical and physical properties of metal nanoparticles make them extremely suitable for developing and designing novel sensing devices, especially electrochemical sensors and biosensors. With their tremendous surface area-to-volume ratio and remarkable small size, metal nanoparticles can provide important functions as catalysts in electrochemical reactions by enhancing electron transfer between electrode surfaces and biomolecules, immobilization and labeling of the biomolecules and even acting as reactants [7]. However, among many nanoparticles Fe_3O_4 nanoparticles (FeNPs) have attracted extensive attention due to their unique multifunctional properties such as small size, biocompatibility, simple and inexpensive fabrication procedure, and low toxicity [8,9].

More recently, conducting polymers have been subject of intense research due to their high conducting exhibition and amazing optical properties. From synthetic point of view, electrochemical methods have been paid special attention to synthesize these polymers due to the high degree of control afforded during the polymerization reaction [10,11]. Therefore, aspartic acid was used in electrode modification to form poly aspartic acid on the Fe_3O_4 nanoparticle surface providing the electrode with top qualities such as preventing loss of the materials from the electrode surface, improving the oxidation currents of the drugs, and improving the anti-interferential ability of the electrochemical sensor. In the pH range of 5–7 PAA (pK_a=3.9) with a carboxylic acid group which did not participate in the polymerization reaction and AA (pK_a=4.10) exist in anionic form, while PRX (pK_a=8.7) and CLO (pKa=9.5) are in cationic form. Thus, under physiological conditions a PAA film strongly repulses anionic uric acid (UA).

Piroxicam (PRX) is a non-steroidal anti-inflammatory drug (NSAID) of the oxicam class used to relieve the symptoms of painful, inflammatory conditions like arthritis. PRX works by preventing the production of a certain type of body chemical called prostaglandins which are involved in the mediation of pain, stiffness, tenderness and swelling [12]. In order to determine the concentration of PRX in biological samples, over the past couple of years, several researchers have developed a variety of methods based on high performance liquid chromatography [13], spectrofluorometry [14], thin layer chromatography [15], capillary electrophoresis [16] and electrochemistry [17,18].

Clopidogrel (CLO) is an oral antiplatelet agent (thienopyridine class) to inhibit blood clots in coronary artery disease, peripheral vascular disease, and cerebrovascular disease. It is a blood-thinning medicine which prevents the platelets in your blood from clotting

(coagulating). Blood clots that form in a blood vessel inside the heart or brain can cause a heart attack or a stroke. CLO is thus used to reduce the risk of heart attacks and strokes in people at high risk including people who have had a heart attack or stroke before and are at risk of getting another one and people with blood circulation problems that may increase their chances of getting a heart attack or stroke. It is marketed by Bristol-Myers Squibb and Sanofi under the trade name Plavix. Literature survey reveals that few analytical methods have been reported for CLO include high performance liquid chromatography [19], gas chromatography-mass spectrometry [20], liquid chromatography-mass spectrometry [21], capillary electrophoresis [22], thin layer chromatography [23], UV spectrophotometry [24], and electrochemistry [25,26].

However, simultaneous consumption of PRX and CLO may lead to greatly increased risk of gastrointestinal bleeding; therefore, simultaneous determination of PRX and CLO would be of crucial importance. Among the analytical methods used for this purpose, the electrochemical techniques are preferred instead due to their simplicity, rapidity and high sensitivity without requirement of long time-consuming sample pretreatments or extractions. To the best of our knowledge, there is no report hitherto published on electrochemical simultaneous determination of PRX and CLO. Therefore, development of a simple, sensitive and accurate analytical method for simultaneous determination of PRX and CLO would be of considerable value.

Statistical design of experiments with its ever-increasing application has recently been employed in optimization of several electrochemical sensors leading to as few experimental runs as possible to obtain the optimum conditions [27,28]. A proper design matrix can lead to obtain a regression equation which highlights the effect of individual factors and their relative importance in a given operation process; thus, increasing the possibility of evaluating the interaction effect between the variables on the response, which is not possible in a classical method [29]. Response surface methodology (RSM) is a combination of mathematical and statistical approaches used for modeling different phenomena and optimizing the experimental results as a function of various parameters. It can weigh existing relationship between a cluster of controlled experimental factors and measured responses according to one or more selected criteria. In addition, orthogonality refers to a matrix design where its elements are orthogonal with each other i.e. correlation coefficients between them are zero except for interactions [30]. However, rotatability, which implies confidence in the predictions, makes the variance of prediction depend only on the scaled distance from the center of the pattern. Since it depends only on the value of distance of each axial point (α), rotatability should be equal to $(2^k)^{1/4}$, where k is number of variables. On the other hand, Central composite design (CCD) is the most popular of many classes of RSM which covers a broad range of experimental domains for effective factors. It requires five levels (+α, +1, 0,

-1, -α) for each factor. The CCD was shown to be highly efficient compared with other designs such as Box-Behnken (BB) and Doehlert Matrix (DM) [31].

In this study, we report the preparation and application of a PAA-FeNPs-MWCNTs/GCE as a novel sensor for nanomolar simultaneous determination of PRX and CLO in the presence of uric acid. The CCD method is used to optimize the experimental variables for the proposed modified electrode. Under optimal conditions, the modified electrode is used to evaluate sensitivity, detection limits and linear dynamic range of the experiments. The analytical performance of the modified electrode in quantification of PRX and CLO in human serum and urine is also profoundly analyzed with satisfactory results.

2. EXPERIMENTAL

2.1. Reagents and solutions

All chemicals were of analytical grade and used without further purification prior to use. CLO standard was kindly provided by Osvah Pharma Company, Iran. Plavix® tablets containing a 75 mg dose of clopidogrel were obtained from local pharmacies. PRX was purchased from Sigma chemical company. MWCNTs were obtained from PlasmaChem GmbH company with a diameter of 5-20 nm and a length of 1-10 µm. Stock standard solutions of 5 mM PRX and 1 mM CLO were freshly prepared in 0.1 M phosphate buffer solution (PB solution) at pH=6.4. All PRX and CLO solutions were prepared by diluting the stock standard solutions using 0.1 M PB solution. Afterwards, electrochemical experiments on PRX and CLO were carried out in 0.1 M PB solution at pH=6.4. Fresh human serum and urine samples were taken from Razi Institute of Vaccine and Serum Company (Tehran, Iran). The human serum and urine samples were filtered and diluted 50 times using a 0.1 M PB solution (pH=6.4) and utilized for the determination of recovery by spiking with PRX and CLO compounds.

2.2. Preparation of the Fe_3O_4 nanoparticles (FeNPs)

FeNPs are prepared via chemical co-precipitation of Fe^{3+} and Fe^{2+} described in the literature [32]. Briefly, $FeCl_2.4H_2O$ (0.9941 g, 5 mmol) and $FeCl_3.6H_2O$ (2.7029 g, 10 mmol) were dissolved in 100 mL of deionized water in a three-necked round bottomed flask (250 mL). The resulting solution is then heated for 1 h at 80°C under N_2 atmosphere. Consequently, 10 mL of concentrated ammonia (25%) were added quickly. After 1 h, the mixture is cooled to room temperature and FeNPs are then isolated by magnetic decantation, washed with distilled water and ethanol, respectively. In the end, the product is dried under vacuum at room temperature (Supplementary data, Fig. S1).

2.3. Synthesis of silica-coated FeNPs (FeNPs@SiO_2)

The FeNPs@SiO_2 core-shell was prepared according to the Stober method [33]. Typically, 500 mg of the synthesized magnetite nanoparticles were dispersed by ultrasonic vibration in a mixture of ethanol (20 mL), deionized water (3 mL) and 1 mL of 25 wt% concentrated aqueous ammonia solution for 20 min. Subsequently, 0.7 mL of tetraethyl orthosilicate (TEOS) was added dropwise. After stirring for 12 h at room temperature under N_2 atmosphere, the products was collected from the solution using a magnet, and then washed several times with water and ethanol and dried at 25 °C under vacuum (Supplementary data, Fig. S1).

2.4. Synthesis of 3-aminopropyl-functionalized FeNPs@SiO_2 (FeNPs@SiO_2-NH_2)

500 mg FeNPs@SiO_2 were dispersed into 50 mL toluene and sonicated for 20 min, followed by the addition of 0.5 mL (3-aminopropyl) triethoxysilane (APTES). Then, the mixture was refluxed at 110 °C with continuous stirring for 12 h under a nitrogen flow. The resulting functionalized FeNPs@SiO_2 was collected by magnetic separation followed by washing with toluene and ethanol several times and drying at 60 °C for 6 h (Supplementary data, Fig. S1).

2.5. Synthesis of poly (succinimide)-functionalized FeNPs (PSI-FeNPs)

The PSI-FeNPs were prepared according to the procedure described in the literature for synthesis of poly (succinimide) with some modifications as follows: 500 mg of FeNPs@SiO_2-NH_2 is dispersed in 85% *o*-phosphoric acid (2 g) in an ultrasonic bath for 20 min, followed by the addition of L-aspartic acid (AA) (1.5 g, 11.3 mmol) [34]. Afterwards, the reaction mixture was stirred for 8 h, under nitrogen atmosphere at 200 °C. The product was dispersed several times in water by ultrasonic vibration and collected by magnetic separation until it was neutral. It was subsequently washed with hot DMSO and with methanol and then was dried at 85 °C under vacuum to yield PSI-FeNPs (Supplementary data, Fig. S1).

2.6. Synthesis of sodium polyaspartate-functionalized FeNPs (PAA-FeNPs)

The hydrolysis of PSI-FeNPs were carried out as follows: 500 mg of FeNPs-PSI were added to 10 mL of NaOH 5% solution and then ultrasonically dispersed for 20 min. After stirring for 1 h at room temperature under N_2 atmosphere, the resulting product was collected by magnetic separation followed by washing with water and ethanol several times and drying at 40 °C for 6 h under reduced pressure (Supplementary data, Fig. S1).

2.7. Instrumentation

All voltammetric measurements were carried out using a PAA-FeNPs-MWCNTs/GCE as the working electrode, an Ag/AgCl/KCl (3M) electrode as the reference electrode and a platinum wire as the auxiliary electrode.

Table 1. Central composite design matrix and its obtained response results

Run order	***Point Type***	***Coded values***			***Real values***			***I_p PRX (µA)***	***I_p CLO (µA)***
		% PAA-FeNPs	***pH***	***t***	***pH***	***t (s)***	***% PAA-FeNPs***		
1	Fact	1	1	1	8.00	60.00	30.00	9.86	10.69
2	Axial	1.68	0	0	9.02	45.00	20.00	9.02	9.92
3	Axial	0	-1.68	0	6.50	19.77	20.00	10.12	11.02
4	Axial	0	0	-1.68	6.50	45.00	3.18	6.22	7.08
5	Fact	-1	1	-1	5.00	60.00	10.00	6.62	7.46
6	Fact	-1	-1	-1	5.00	30.00	10.00	5.68	6.76
7	Fact	1	-1	-1	8.00	30.00	10.00	7.86	8.87
8	Axial	-1.68	0	0	3.98	45.00	20.00	5.37	6.24
9	Axial	0	0	1.68	6.50	45.00	36.82	9.35	10.27
10	Fact	1	1	-1	8.00	60.00	10.00	9.63	10.46
11	Axial	0	1.68	0	6.50	70.23	20.00	12.75	13.52
12	Center	0	0	0	6.50	45.00	20.00	12.49	13.41
13	Fact	-1	-1	1	5.00	30.00	30.00	7.37	8.20
14	Center	0	0	0	6.50	45.00	20.00	12.61	13.49
15	Fact	1	-1	1	8.00	30.00	30.00	8.95	9.77
16	Center	0	0	0	6.50	45.00	20.00	12.25	13.05
17	Fact	-1	1	1	5.00	60.00	30.00	9.54	10.43

The differential pulse voltammetry (DPV), cyclic voltammetry (CV) and chronoamperometry (CA) experiments were conducted using an Autolab PGSTAT 30 Potentiostat Galvanostat (EcoChemie, The Netherlands) coupled with a 663 VA stand

(Metrohm Switzerland). All potentials are given with respect to the potential of the reference electrode. A Metrohm 744 pH meter using a combination glass electrode was used for pH measurements. The morphological analyses were carried out by using MIRA3 TESCAN scanning electron microscope (SEM). Fourier transform infrared (FTIR) spectra were recorded from KBr disks on a Galaxy series 5000 spectrometer. The statistical computer package of Design-Expert 7.0.0 (Stat-Ease Inc., Minneapolis) was used by a PC for regression analysis of obtained data and estimation of the coefficients of regression.

2.8. Central composite design as an optimization approach

In the current study, optimization in determination of PRX and CLO at a PAA-FeNPs-MWCNTs/GC electrode was carried out using a CCD as a RSM. To predict the mathematical relationship between independent factors and dependent response via CCD matrix design, a second order polynomial model was fitted to the experimental results. Then, a total of 17 experiments were performed based on a 2^3 full factorial CCD, consisting of 8 factorial points (coded to the usual ±1 notation), 6 axial points (±α, 0, 0), (0, ±α, 0), (0, 0, ±α) and 3 replicates at the center points (0, 0, 0) to verify any change in estimation procedure (Table 1).

2.9. Preparation of the modified electrode

Prior to modification, the GCE (2 mm diameter, Metrohm) was first polished with 0.3 and 0.05 μm aluminum oxide slurry and rinsed thoroughly with triply distilled water. The electrode was then cleansed by sonication for 5 min, in ethanol and distilled water, successively and then dried under a nitrogen gas flow. The amount PAA-FeNPs in the modifier matrix not only greatly influenced the sensitivity of the sensor but also significantly increased selectivity of the modified electrode against interfering UA. Therefore, the optimum composition of 21.6% PAA-FeNPs (suggested by the optimization software) was chosen for the fabrication of the modified electrode. A stock solution of PAA-FeNPs-MWCNTs in DMF was prepared by dispersing 1.568 mg MWCNTs and 0.432 mg PAA-FeNPs (78.4%:21.6% w/w) in 2 mL dimethyl formamide (DMF) using ultrasonic bath in order to achieve a homogeneous solution. Thereafter, 20 μL of prepared suspension was cast on the electrode with a micro syringe and left to dry at room temperature to obtain the modified electrode. Finally, the fabricated PAA-FeNPs-MWCNTs/GCE was placed in the electrochemical cell containing 0.1M PB solution. Then, it was subjected to 10 cycles in the potential window of 0.0 to 1.0 V using the CV method to obtain stable responses.

2.10. General procedure

Each sample solution (10 mL) containing appropriate amounts of PRX and CLO in 0.1M PB solution at pH of 6.4 were transferred into the voltammetric cell. The differential pulse voltammograms were recorded by applying a positive-going potential from 0.10 to 0.85 V. The voltammograms showed anodic peaks around 0.38 and 0.69 V corresponding to the PRX and CLO compounds, respectively. Calibration curves were obtained by plotting the anodic peak currents of PRX and CLO against the corresponding concentrations. After each measurement, the PAA-FeNPs-MWCNTs/GCE was regenerated by thoroughly washing the electrode with triply distilled water and then 5% sodium hydroxide solution to remove all materials which had been absorbed on the electrode surface. In the end, the electrode was thoroughly rinsed with distilled water to provide a fresh clean surface for the next experiment.

3. RESULTS AND DISCUSSION

3.1. Characterization of the PAA-FeNPs-MWCNTs composite

Fig.1a and 1b show the SEM images of the typical MWCNTs and PAA-FeNPs, respectively. As it can be seen, the particle sizes of PAA-FeNPs are between 20 to 50 nm.

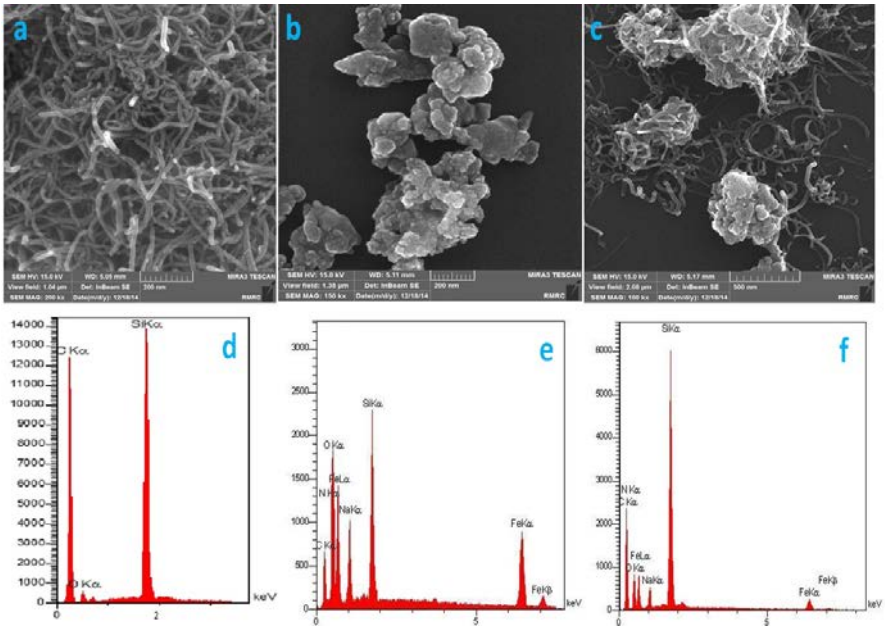

Fig. 1. SEM micrographs of the samples: (a) MWCNTs; (b) PAA-FeNPs and (c) PAA-FeNPs-MWCNTs and SEM-EDX spectrum of the samples: (d) MWCNTs; (e) PAA-FeNPs and (f) PAA-FeNPs-MWCNTs

The SEM image of the PAA-FeNPs-MWCNTs (Fig.1c) shows that the PAA-FeNPs surface was covered with MWCNTs. The porosity of PAA-FeNPs leads to an increase in the surface area of the composite; therefore, enhancement in the electrical response of the as-modifiied electrode can be expected. The EDX analysis of the MWCNTs shows presence of C, O and Si (Fig. 1d) while as of PAA-FeNPs it shows presence of C, N, O, Fe, Na and Si peaks (Fig. 1e). Moreover, Fig. 1f shows elemental EDX analysis of PAA-FeNPs-MWCNTs composite that shows the presence of C, N, O, Fe, Na and Si peaks confirming the correct composition for a PAA-FeNPs-MWCNTs composite. The high percentage of Si is due to the Si in the base plate originated from pyrolized photoresist film (PPF).

The electro-active surface area of the modified electrodes was assessed by CV in 0.1 M PB solution (pH 7.0) containing 4 mM potassium ferricyanide at GCE, MWCNTs/GCE, PAA-FeNPs/GCE and PAA-FeNPs-MWCNTs/GCE. $K_3Fe(CN)_6$ exhibited a pair of reversible redox peaks at a bare and modified GCE. The redox peak currents for the modified electrodes were larger than those for an unmodified GCE. On the other hand, under the same conditions, the anodic peak currents were linear with the square root of scan rate (in the range of 10-200 mVs^{-1}) on the GCE and other modified GC electrodes. The obtained regression equations for the four electrodes are as follows:

I_{pa} (μA)=28.74 $v^{1/2}$ $(V\ s^{-1})^{1/2}$ + 4.240 (R^2=0.994) GCE
I_{pa} (μA)=550.9 $v^{1/2}$ $(V\ s^{-1})^{1/2}$ + 24.40 (R^2=0.993) MWCNTs/GCE
I_{pa} (μA)=209.8 $v^{1/2}$ $(V\ s^{-1})^{1/2}$ + 14.39 (R^2=0.991) PAA-FeNPs/GCE
I_{pa} (μA)=609.3 $v^{1/2}$ $(V\ s^{-1})^{1/2}$ + 21.67 (R^2=0.995) PAA-FeNPs-MWCNTs/GCE

A reversible system should satisfy the Randles-Sevcik equation [35]:

$$I_p = (2.69\times10^5)\ n^{3/2}\ A\ C_o\ D^{1/2}\ \nu^{1/2}$$

Where I_p (A) is the peak current of the CV, n is the number of electrons transferred in redox reaction, A (cm^2) is the electro-active surface area of the electrode, D ($cm^2\ s^{-1}$) is the diffusion coefficient of the redox probe ($K_3[Fe(CN)_6]$) in the bulk solution (0.1 M PB solution, pH=7), C_o (mol cm^{-3}) is the concentration of redox probe and ν ($V\ s^{-1}$) is the scan rate.By application of the above equation and comparison of the slopes of the equations with respect to that of the bare GCE, the apparent electro-active surface areas of the PAA-FeNPs-MWCNTs/GCE, PAA-FeNPs/GC and MWCNTs/GC modified electrodes were estimated to be 21.2, 7.3 and 19.2 times as large as that of the unmodified GC electrode, respectively. It can be concluded that the application of the PAA-FeNPs-MWCNTs composite can lead to a higher electro-active surface area than that of each composite.

3.2. Electrochemical behavior of PRX and CLO on PAA-FeNPs-MWCNTs/GCE

The electrochemical behavior of a mixture of 30 μM PRX and 20 μM CLO was investigated using CV at PAA-FeNPs-MWCNTs/GC electrodes (Supplementary data, Fig. S2). PRX and CLO showed irreversible oxidation peaks at pH of 6.4. Fig. 2 shows the differential pulse voltammograms of a solution of 30 μM PRX and 20 μM CLO in the presence of 100 μM UA both at bare and modified GC electrodes. The voltammograms were recorded for PRX and CLO at (a) GCE, (b) PAA-FeNPs/GCE, (c) MWCNTs/GCE and (d) PAA-FeNPs-MWCNTs/GCE. As can be seen (curve a in Fig. 2) small oxidation peak currents for PRX and CLO can be observed at an unmodified GCE. The oxidation peak currents of PRX and CLO further increased and slightly shifted to less positive potentials at the PAA-FeNPs/GCE with respect to the GCE associating electro-catalytic effects of PAA-FeNPs (curve b in Fig. 2). The MWCNTs/GCE significantly enhanced the corresponding oxidation peak currents of PRX and CLO compared with the bare GCE (curve c in Fig. 2) which can be related to the high surface area of MWCNTs. The oxidation peak currents of PRX and CLO showed the highest values at the PAA-FeNPs-MWCNTs/GCE (curve d in Fig. 2) with respect to those from the MWCNTs/GCE, conclusively evidencing the synergistic electro-catalytic effects of the PAA-FeNPs-MWCNTs composite.

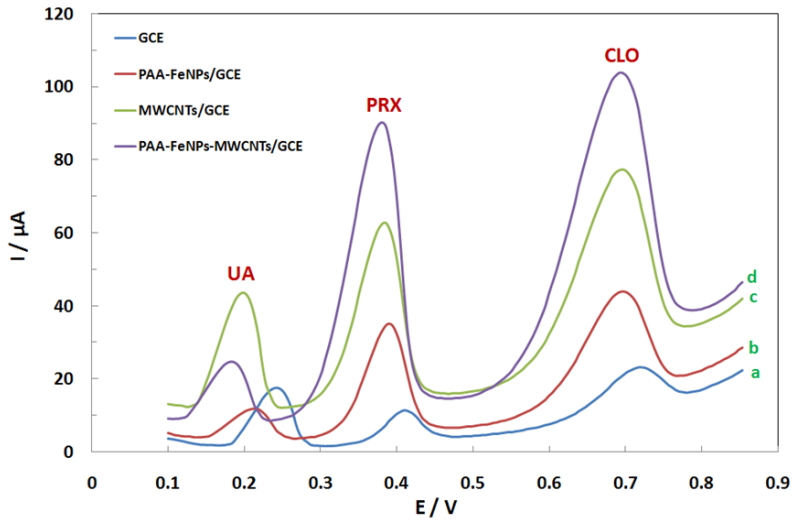

Fig. 2. Differential pulse voltammograms of 30 μM PRX and 20 μM CLO at (a) GCE, (b) PAA-FeNPs/GCE, (c) MWCNTs/GCE and (d) PAA-FeNPs-MWCNTs/GCE in 0.1 M PB solution (pH=6.4) contain 100 μM UA. Other conditions: Open circuit, tacc=51.1 s, pulse amplitude=50 mV, scan rate=10 mV s^{-1}, interval time 0.5 s, modulation time =0.2 s and step potential=5 mV

In addition, higher oxidation peak currents could be attributed to the large surface area of the composite film which is in accordance with previous results in section 3.1. On the other

hand, the decreasing in oxidation peak currents of UA at PAA-FeNPs-MWCNTs/GCE with respect to those from the MWCNTs/GCE are clear evidences of the negative charge of PAA-FeNPs. Due to proton release from PAA, PAA-FeNPs have negative charge at such a pH leading to increased selectivity of the modified electrode against interfering compounds (e.g. UA).

3.3. Optimization of experimental variables by central composite design (CCD)

In CCD optimization, a central composite design with three replicates at the center point was used to identify the effect of individual variables and their interactions on response. Design-Expert software was used for statistical evaluation of the experimental conditions of CCD.

Table 2. Analysis of variance for PRX after removing insignificant effects

Source	***Sum of Squares***	***DF***	***Mean Square***	***F Value***	***p-value***
Model	92.356	7	13.194	84.085	< 0.0001
pH	12.814	1	12.814	81.663	< 0.0001
t	7.638	1	7.638	48.676	< 0.0001
% PAA-FeNPs	9.175	1	9.175	58.475	< 0.0001
(pH)*(%PAA-eNPs)	1.353	1	1.353	8.623	0.0166
$(pH)^2$	42.676	1	42.676	271.979	< 0.0001
$(t)^2$	2.248	1	2.248	14.329	0.0043
$(\%\ PAA\text{-}FeNPs)^2$	34.016	1	34.016	216.787	< 0.0001
Residual	1.412	9	0.157		
Lack of Fit	1.345	7	0.192	5.718	0.1569
Pure Error	0.067	2	0.034		

Responses are presented in Table 1 where actual (natural scale) and coded (dimensionless scale) values were tabulated separately. Three factors of PAA-FeNPs amount in the modifier

matrix (%PAA-FeNPs), solution pH, and accumulation time (t) were selected as operational (independent) variables while oxidation peak current of PRX and CLO were considered as responses. Identical amounts of PRX and CLO solution (5 µM of PRX and 4 µM CLO) were injected for three times in each experimental condition of CCD. A second order polynomial model was fitted to experimental results in order to predict the mathematical relationship between independent factors and the dependent response in accordance with the CCD matrix design. To verify whether the main effects are significant, an analysis of variance (α=5%) was conducted. Tables S1 and S2 show the analysis of variance for the suggested model before removing insignificant effects for PRX and CLO, respectively.

Table 3. Analysis of variance for CLO after removing insignificant effects

Source	***Sum of Squares***	***DF***	***Mean Square***	***F Value***	***p-value***
Model	89.977	7	12.854	69.032	< 0.0001
pH	12.622	1	12.622	67.785	< 0.0001
t	6.811	1	6.811	36.579	0.0002
% PAA-FeNPs	8.708	1	8.708	46.764	< 0.0001
(pH)*(%PAA-eNPs)	1.345	1	1.345	7.222	0.0249
$(pH)^2$	42.188	1	42.188	226.574	< 0.0001
$(t)^2$	2.314	1	2.314	12.430	0.0065
$(\%\ PAA\text{-}FeNPs)^2$	33.512	1	33.512	179.976	< 0.0001
Residual	1.676	9	0.186		
Lack of Fit	1.566	7	0.224	4.072	0.2113
Pure Error	0.110	2	0.055		

It can be concluded from these Tables that the tow terms of interactions, (%PAA-FeNPs)×(t) and (pH)×(t), were insignificant; therefore, these factors were removed from the model. On the other hand, Tables 2 and 3 show the analysis of variance for the suggested model after removing insignificant effects.

By applying regression analysis to the experimental data, the CCD results were fitted with a polynomial equation. For PRX, the most appropriate empirical relationships between responses and input variables after removing insignificant effects in coded values were expressed by the following quadratic models:

$$I_p(\mu A)=+12.48+0.97\times(pH)+0.75\times(t)+0.82\times(\%PAA\text{-}FeNPs)-0.41\times(pH)\times(\%PAA\text{-}FeNPs)-1.95\times(pH)^2-0.45\times(t)^2-1.74\times(\%PAA\text{-}FeNPs)^2 \qquad PRX$$

For CLO, the empirical relationships between responses and input variables after removing insignificant effects in coded values were expressed by the corresponding quadratic models:

$$I_p(\mu A)=+13.34+0.96\times(pH)+0.71\times(t)+0.80\times(\%PAA\text{-}FeNPs)-0.41\times(pH)\times(\%PAA\text{-}FeNPs)-1.93\times(pH)^2-0.45\times(t)^2-1.72\times(\%PAA\text{-}FeNPs)^2 \qquad CLO$$

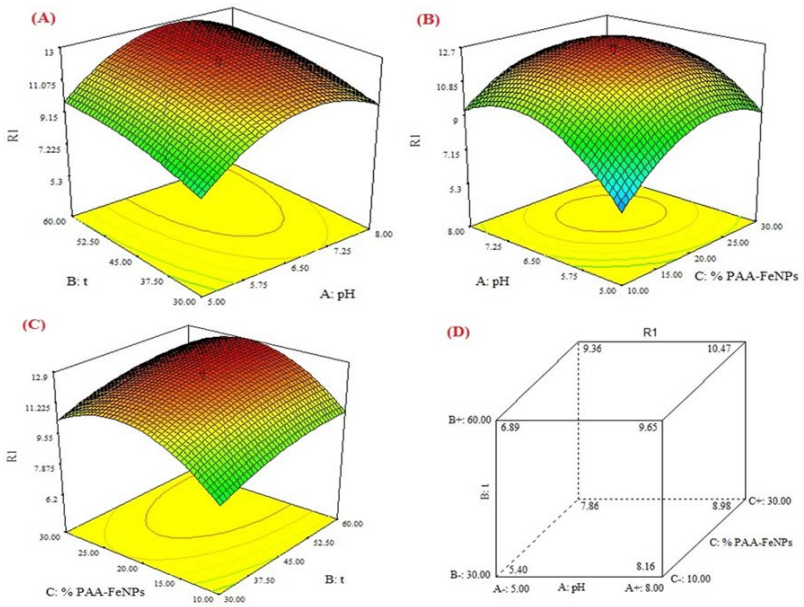

Fig. 3. Three-dimensional response surface plot for the effect of (A) pH and t, (B) pH and % PAA-FeNPs, (C) t and % PAA-FeNPs, (D) % PAA-FeNPs, pH and t, on the peak height of 5 μM PRX

Figs. 3, 4 show three-dimensional response surface plots for relationship between PAA-FeNPs amount in modifier matrix (%PAA-FeNPs), pH of solution (pH) and accumulation time (t) on the peak current of the PRX and CLO oxidations. Contour plots for %PAA-FeNPs, pH and t are showed in supplementary data (Figs. S3 and S4).

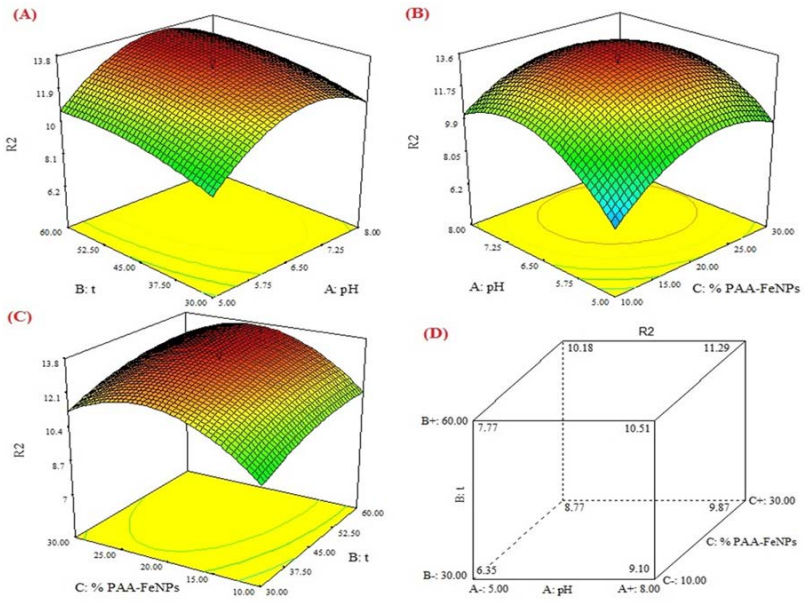

Fig. 4. Three-dimensional response surface plot for the effect of (A) pH and t, (B) pH and % PAA-FeNPs, (C) t and % PAA-FeNPs, (D) % PAA-FeNPs, pH and t, on the peak height of 4 μM CLO

The ultimate goal in optimization is to achieve the maximum responses for PRX and CLO and to select the factors which are within the range. Optimization was carried out using the Design-Expert software. It starts with a small value of a penalty function in a downhill simplex (Nelder-Mead) multi-dimensional pattern search for minimization or maximization of an objective function [36]. The results of this non-linear optimization method are shown in supplementary data (Fig. S5). According to which the optimum values of the main factors revealed to be 21.6% of the PAA-FeNPs amount in the modifier matrix, 6.4 of solution pH and 51.1 s of accumulation time.

3.4. Effects of the scan rate

The effect of potential scan rates on the oxidation responses of 15 μM PRX and 10 μM CLO were explored using the CV method over the range of 10-160 mVs^{-1} (Fig. 5). The linear relationships between the anodic peak currents and scan rates were observed for PRX and CLO in the range of 10-70 mVs^{-1} as follows:

$I_{pa}(\mu A)=0.473\nu\ (mV\ s^{-1})+0.605$	(R^2 =0.997)	PRX
$I_{pa}(\mu A)=0.385\nu\ (mV\ s^{-1})+0.921$	(R^2=0.997)	CLO

The linear relationship between peak currents and scan rates suggests that the oxidation reactions of two compounds at PAA-FeNPs-MWCNTs/GCE are adsorption-controlled processes at such scan rates. The linear relationships between the anodic peak currents and

square root of scan rates were observed to be in the range of 80-160 mVs^{-1} for PRX and CLO as follows:

$I_{pa}(\mu A)=4.813\nu^{1/2}$ (mV s^{-1}) $^{1/2}$+ 2.108 (R^2=0.996) PRX

$I_{pa}(\mu A)=2.997\nu^{1/2}$ (mV s^{-1}) $^{1/2}$+ 2.667 (R^2=0.998) CLO

The linear relationship between peak currents and square root of scan rates indicates that the oxidation reactions of the two compounds at PAA-FeNPs-MWCNTs/GCE are diffusion controlled at such scan rates.

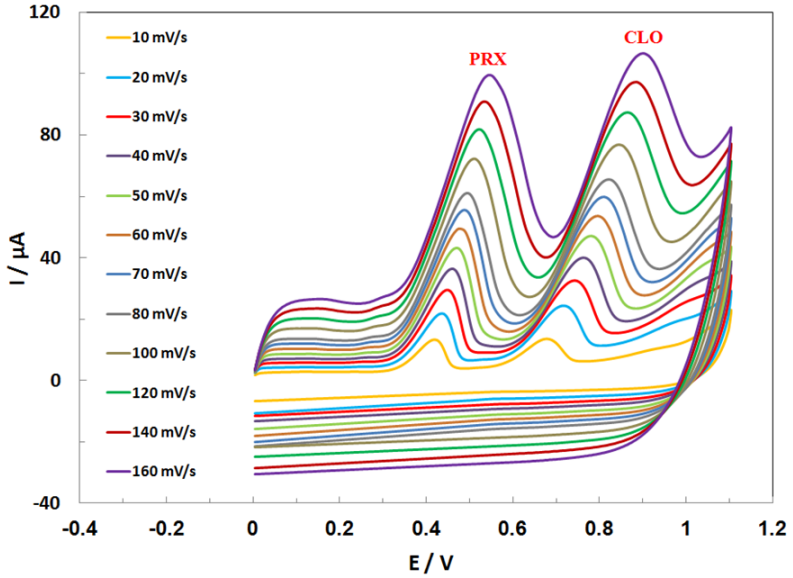

Fig. 5. Effect of scan rate on the cyclic voltammograms peak currents of 15 µM of PRX and 10 µM of CLO in phosphate buffer (pH=6.4) solution for different scan rate

3.5. Linear dynamic range and detection limit of the method

The electrochemical responses of simultaneous determinations of PRX and CLO in a 0.1M PB solution of pH 6.4 using PAA-FeNPs-MWCNTs/GCE are depicted in Figs.6 and 7. Fig.6 shows differential pulse voltammograms for various concentrations of PRX and CLO at PAA-FeNPs-MWCNTs/GCE in the presence of 100 µM UA. A linear dynamic range from 0.2 µM to 80 µM with a calibration equation of I_p (µA)=2.0173C (µM)+1.0265 (R^2=0.9989) and a detection limit of 45 nM (S/N=3) were obtained for PRX. For CLO, a linear dynamic range from 0.4 µM to 48 µM with a calibration equation of I_p (µA)=2.3882C (µM)+1.3361 (R^2=0.9964) and a detection limit of 76 nM (S/N=3) were obtained. Further investigations demonstrated that these linear ranges were kept constant in mixed solutions of PRX and CLO revealing high efficiency of the fabricated modified electrode for simultaneous determinations of these compounds in mixed pharmaceutical samples.

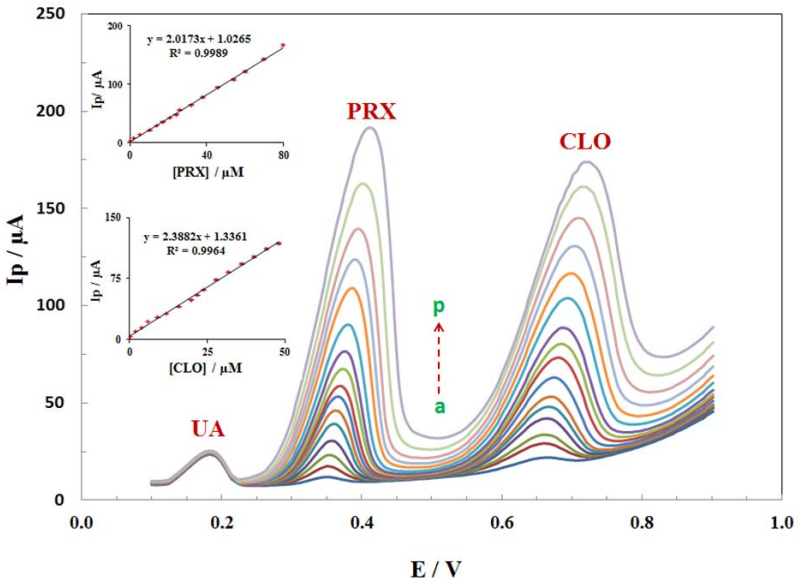

Fig. 6. Differential pulse voltammograms for different concentrations of PRX and CLO mixtures in 0.1 M PB solution (pH=6.4) contain 100 µM UA at optimum conditions as (a) 0.2+0.4, (b) 2+2, (c) 5+4, (d) 10+6, (e) 14+9, (f) 17+12, (g) 21+16, (h) 24+20, (i) 26+22, (j) 32+24, (k) 38+28, (l) 46+32, (m) 54+36, (n) 60+40, (o) 70+44 and (p) 80+48, respectively, in which the first value is the concentration of PRX in µM and the second value is the concentration of CLO in µM

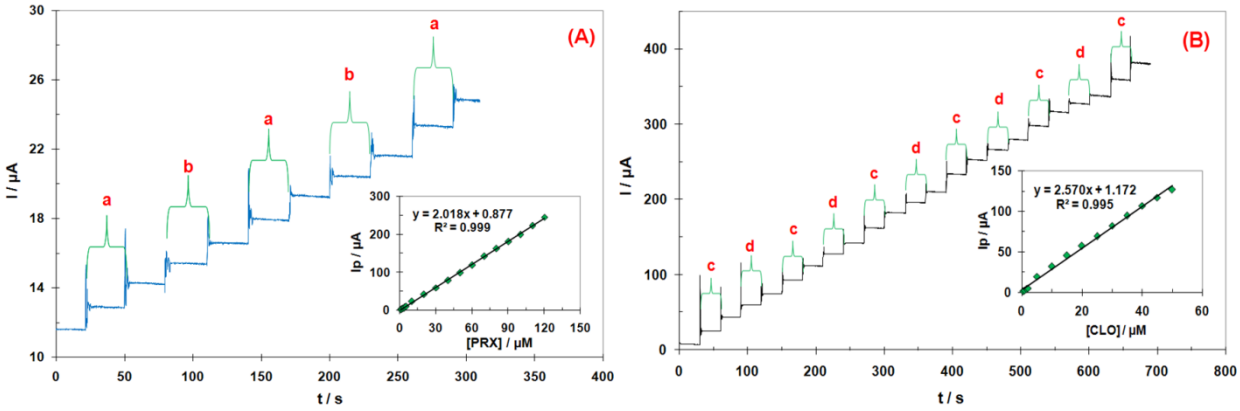

Fig. 7. Hydrodynamic amperometric response at rotating PAA-FeNPs-MWCNTs/GCE (rotating speed 3000 rpm) held at 0.8 V in PB solution (pH=6.4) contain 100 µM UA for successive additions in µM of (a) 0.8 PRX, (b) 0.5 CLO, (c) 10 PRX and (d) 5 CLO

Fig.7 displays two chronoamperograms of the response of a rotated modified electrode (3000 rpm) following the successive injection of PRX and CLO at an applied potential of 0.8 V in PB solution (pH=6.4) containing 100 µM UA. For PRX, the linear dynamic range was from 0.8 µM to 120 µM, with a calibration equation of I_p (µA)=2.018C (µM)+0.877 (R^2=0.999) and a detection limit of 0.096 µM (S/N=3) was obtained, and for CLO the linear

dynamic range was from 0.5 µM to 50 µM, with a calibration equation of I_p(µA)=2.570C (µM)+1.172 (R^2=0.995) and a detection limit of 0.075 µM (S/N=3) was obtained.

Table 4. Comparison of various electrochemical methods for detection of PRX and CLO

Type of determination	**Analyte**	**Electrode**	**LDR (µM)**	**DL (µM)**	**Sensitivity (µA/µM)**	**Ref.**
Individual	***PRX***	MWCNTs-NHNPs/GCE	0.7-75	0.11	1.765	[17]
		MWCNTs-NHNPs-MCM-41/GCE	0.1-70	0.04	2.020	[18]
	CLO	Chemically modified carbon paste sensors	0.1-10000	0.034	No Report	[25]
		gold electrode	0.99-2.9	0.36	No Report	[26]
Simultaneous	***PRX***	PAA-FeNPs-MWCNTs/GCE	0.2-80	0.045	2.017	This work
	CLO		0.4-48	0.076	2.389	

The analytical figure of merits for determination of individual PRX and CLO in previous reports were compared with our proposed method as shown in Table 4. It can be seen that the present method can provide the high sensitivity and the low detection limit in simultaneous determination of PRX and CLO. In addition our literature survey showed that this is the first report on simultaneous electrochemical determination of PRX and CLO.

Table 5. Maximum tolerable concentration of interfering species

Interfering species	***PRX***	***CLO***
	C_{int}* / (µM)*	C_{int} / (µM)*
Ascorbic acid	140	180
Uric acid	100	110
L-Glutamic acid	300	350
L-Alanin	450	400
Aspartic acid	250	200
L-histidine	500	400
Dopamine	120	100
Tryptophan	110	170

*C_{int} refers to interfering compound concentration

3.6. Repeatability and long-term stability of the electrode

The repeatability of the analytical signals was studied and relative standard deviations (RSD) of 1.3% and 1.2 % for ten consecutive determinations of 10 µM PRX and 10 µM CLO were obtained, respectively. The results confirmed good repeatability of the proposed electrode at the optimum conditions.

The modified electrode has a further attraction of good long-term stability. It was tested by measuring the decrease in voltammetric current during the repetitive DPV measurements of PRX and CLO solutions with PAA-FeNPs-MWCNTs/GCE which was stored in solution (wet condition) or exposed to the atmosphere (dry condition) for a certain period of time. For example, under wet condition storage for 36 h the electrode showed less than 4.1 and 3.8% decrease in the voltammetric oxidation peak current of 10 µM PRX and 10 µM CLO in 0.1 M PB solution (pH=6.4), respectively.

When the electrode was stored under dry conditions for 7 days, the oxidation peak current of PRX and CLO in solution was reduced less than 4.9 and 4.2%, respectively. The results confirmed excellent long-term stability of the modified electrode as a sensor for determination of PRX and CLO.

3.7. Interference studies

The influences of common interfering species in the presence of 10 µM PRX and 10 µM CLO were investigated under optimum conditions (Table 5).

Table 6. Determination of PRX and CLO in human serum and urine with PAA-FeNPs-MWCNTs/GCE

Sample	***Spiked/ µM***		***Found / µM***		***RSD[a]/%***		***Recovery %***	
	PRX	***CLO***	***PRX***	***CLO***	***PRX***	***CLO***	***PRX***	***CLO***
Blood	2.00	2.00	2.044	2.059	3.2	2.9	102.2	103.0
	5.00	5.00	4.924	4.973	2.1	2.0	98.5	99.5
	10.00	10.00	9.863	10.485	1.4	1.3	98.6	104.8
Urine	2.00	2.00	1.972	1.945	2.7	2.8	98.6	104.6
	5.00	5.00	4.889	5.059	2.0	2.0	97.8	101.2
	10.00	10.00	10.126	9.761	1.3	1.4	101.3	97.6

[a] Average of five determinations at optimum conditions

The results confirmed that interfering species did not significantly influence the height of the peak currents for PRX and CLO. The tolerance limits are defined as the concentrations which give an error of ≤ 10%. The results indicated that the proposed method is free from interferences of the most common interfering agents.

3.8. Real sample analysis

The applicability of a PAA-FeNPs-MWCNTs/GCE to the determination of PRX and CLO in human serum and human urine as the real samples was examined. Differential pulse voltammograms were obtained by spiking prepared real solutions with appropriate samples and applying PAA-FeNPs-MWCNTs/GCE under optimal conditions. To avoid any matrix effect, standard addition method was employed in the calculation of the concentrations of PRX and CLO. The results are shown in Table 6. The recoveries indicate that both the accuracy and repeatability of the proposed method are perfectly acceptable. The experimental results confirmed that under the optimum conditions the proposed electrode has great potential for the determination of trace amounts of PRX and CLO in biological systems or pharmaceutical preparations.

4. CONCLUSIONS

In this report, the new application of a novel sensor is introduced for simultaneous determination of PRX and CLO based on a PAA-FeNPs-MWCNTs composite modified glassy carbon electrode. In order to reduce the number of experiment required to discover the optimum conditions of the analysis, CCD was applied as a response surface approach. The results showed that combination of PAA-FeNPs and MWCNTs as a composite in the modified electrode under optimum conditions can lead to very high sensitivity for the simultaneous determination of PRX and CLO due to an excellent electro-catalytic performance and high electro-active surface area of the composite. In addition, the negative charge of the modified electrode surface at pH of 6.4 can increase selectivity of the proposed method. The interfering study of some common species showed no significant interference in the simultaneous determination of PRX and CLO. Application of the proposed sensor for the determination of PRX and CLO in some real samples showed satisfactory results, without the necessity of sample pretreatments or time-consuming extractions. The simple fabrication procedure, high sensitivity, excellent selectivity, good reproducibility and high speed suggest that the proposed sensor is an attractive candidate for practical applications.

Acknowledgments

The authors gratefully acknowledge the research council of Arak University for providing financial support (No. 92.9829) for this work. Special thanks to Professor A.J. McQuillan from Otago University in New Zealand for his valuable comments on this work.

REFERENCES

[1] A. Babaei, M. Babazadeh, and M. Afrasiabi, Chin. J. Chem. 29 (2011) 2157.
[2] A. Asghari, S. Kianipour, M. Afrasiabi, and M. Rajabi, Sensor Lett. 11 (2013) 545.
[3] A. B. Moghaddam, M. R. Ganjali, R. Dinarvand, P. Norouzi, A. A. Saboury, and A. A. Moosavi-Movahedi, Biophys. Chem. 128 (2007) 30.
[4] A. Babaei, A. Yousefi, M. Afrasiabi, and M. Shabanian, J. Electroanal. Chem. 740 (2015) 28.
[5] M. Afrasiabi, and S. Kianipour, Anal. Bioanal. Electrochem. 7 (2012) 331.
[6] A. Babaei, M. Farshbaf, M. Afrasiabi, and A. Dehdashti, Anal. Bioanal. Electrochem. 6 (2012) 564.
[7] A. Babaei, M. Afrasiabi, and G. Azimi, Anal. Methods 7 (2015) 2469.
[8] X. Liu, H. Zhu, and X. Yang, Talanta 87 (2011) 243.
[9] D. Lu, Y. Zhang, L. Wang, S. Lin, C. Wang, and X. Chen, Talanta 88 (2012) 181.
[10] P. Pickup, W. Kutner, C. Leidner, and R. W. Murray, J. Am. Chem. Soc. 106 (1984) 1991.
[11] E. P. Krinichnaya, A. P. Moravsky, O. Efimov, J. W. Sobczak, K. Winkler, W. Kutner, and A. L. Balch, J. Mater. Chem. 15 (2005) 1468.
[12] A. Gilman, and L. Goodman, Goodman and Gilman's, The Pharmacological Basis of Therapeutics, 11th ed., Vol. 2 (Eds: L. Brunton, J. Lazo, K. Parker), McGraw-Hill Professional, New York (2005), pp. 669 –674.
[13] P. Heizmann, J. Körner, and K. Zinapold. J. Chromatogr. B Biomed. Sci. Appl. 374 (1986) 95.
[14] G. M. Escandar, Analyst 124 (1999) 587.
[15] S. P. Puthli, and P. R. Vavia, J. Pharm. Biomed. Anal. 22 (2000) 673.
[16] M. Fillet, I. Bechet, V. Piette, and J. Crommen, Electrophoresis 20 (1999) 1907.
[17] A. Babaei, M. Sohrabi, and M. Afrasiabi, Electroanalysis 12 (2012) 2387.
[18] A. Babaei, and M. Afrasiabi, Ionics 21 (2015) 1731.
[19] S. S. Singh, K. Sharma, D. Barot, P. R. Mohan, and V. B. Lohray, J. Chromatogr. B 821 (2005) 173.
[20] P. Lagorce, Y. Perez, J. Ortiz, J. Necciari, and F. Bressolle, J. Chromatogr. B 720 (1998) 107.
[21] H. Ksycinska, P. Rudzki, and M. B. Kiliszek, J. Pharm. Biomed. Anal. 41 (2006) 533.

[22] A. S. Fayed, S. A. Weshahy, M. A. Shehata, N. Y. Hassan, J. Pauwels, J. Hoogmartens, and A. Van Schepdael, J. Pharm. Biomed. Anal. 49 (2009) 193.
[23] H. Agrawal, N. Kaul, A. R. Paradkar, and K. R. Mahadik, Talanta 61 (2003) 581.
[24] H. E. Zaazaa, S. S. Abbas, M. Abdelkawy, and M. M. Abdelrahman, Talanta 78 (2009) 874.
[25] A. F. Khorshid, J Bioproces. Biotechnic. 4 (2014) 1.
[26] A. R. Mladenovic, V. M. Jovanovic, S. D. Petrovic, D. Z. Mijin, S. Z. Drmanic, and M. L. Avramovivic, J. Serb. Chem. Soc. 78 (2013) 2131.
[27] J. Zolgharnein, T. Shariatmanesh, and A. Babaei, Sens. Actuators, B Chem. 186 (2013) 536.
[28] J. Zhou, X. Yu, C. Ding, Z. Wang, Q. Zhou, H. Pao, and W. Cai, J. Environ. Sci. 23 (2011) 22.
[29] D. C. Montgomery, Design and Analysis of Experiments, 5n ed., John Wiley & Sons, New York (2001).
[30] T. P. Ryan, Modern Experimental Design, John Wiley & Sons, Inc., Hoboken, NJ, USA (2007).
[31] J. Zolgharnein, A. Shahmoradi, and J. B. Ghasemi, J. Chemomet. 27 (2013) 12.
[32] K. Can, M. Ozmen, and M. Ersoz, Colloids Surf. B 71 (2009) 154.
[33] W. Stober, A. Fink, and E. J. Bohn, J. Colloid Interface Sci. 26 (1968) 62.
[34] T. Nakato, A. Kusuno, and T. Kakuchi, J. Polym. Sci. Part A 38 (2000) 117.
[35] A. J. Bard, and L. R. Faulkner, Electrochemical Methods, Fundamentals and Applications, 2n ed., Wiley, New York (2001), pp. 229-231.
[36] M. Jalali-Heravi, H. Parastar, and H. Ebrahimi-Najafabadi, J. Chromatogr. A 1216 (2009) 6088.